Cancer Chemother Pharmacol (2004) 54: 249–258
DOI 10.1007/s00280-004-0806-1

ORIGINAL ARTICLE

James W. Darnowski · Frederick A. Goulette
Leslie P. Cousens · Devasis Chatterjee · Paul Calabresi

Mechanistic and antineoplastic evaluation of taurolidine in the DU145 model of human prostate cancer

Received: 22 October 2003 / Accepted: 26 February 2004 / Published online: 2 June 2004

Abstract Taurolidine (TRD) was designed in the 1970s as a broad-spectrum antibiotic and is used clinically at high doses without systemic toxicity. We have found that this agent possesses cytotoxic activity in human tumor cell lines and antineoplastic activity in mice bearing i.p. human tumor xenografts. We now report the mechanism by which TRD induces cell death in DU145 human prostate tumor cells. The IC_{50} (3 days) of TRD in this model was 16.8 ± 1.1 μ*M*. Cytotoxicity was associated with DNA debris and increased membrane phosphatidylserine externalization, both suggesting the induction of apoptosis. This was confirmed by the ability of TRD to induce PARP cleavage in these cells, an effect prevented by coexposure to the pan-caspase inhibitor zVAD-FMK. TRD exposure also resulted in the appearance of cytochrome *c* in the cytoplasm, procaspase 9 activation within 2 h of drug exposure and procaspase 8 activation 4 h after exposure. Parallel experiments revealed that cytochrome *c*appearance in the cytoplasm was not blocked by preexposure to zVAD-FMK, while activation of both procaspase 9 and procaspase 8 was prevented. Finally, antineoplastic activity was assessed in mice bearing subcutaneous xenografts of DU145 cells. Initial studies quantitated the toxicity of three i.p. injections of TRD, administered as one injection on three alternate days per week, at doses ranging from 500 to 700 mg/kg per injection. The 500 mg/kg dose produced about 7% mortality after three cycles and effectively inhibited tumor growth. Thus, TRD induced mitochondrial-mediated apoptosis in DU145 human prostate tumor cells and this effect could be exploited for therapeutic advantage.

J. W. Darnowski (✉) · F. A. Goulette · L. P. Cousens
D. Chatterjee · P. Calabresi
Department of Medicine,
Divisions of Clinical Pharmacology and Medical Oncology,
Brown University and Rhode Island Hospital,
593 Eddy Street, Providence, RI 02903, USA
E-mail: jdarnowski@lifespan.org
Tel.: +1-401-4445087
Fax: +1-401-4448483

Keywords Taurolidine · Apoptosis · Cytochrome *c* · Chemotherapy · Prostate cancer · Xenografts

Abbreviations ANT: Adenine nucleotide translocator · IC_{50}: The concentration of drug required to inhibit cell growth by 50% compared to nondrug-treated controls · Fas: CD95/Apo-1 · i.p.: Intraperitoneal · MTD: Maximally tolerated dose · PARP: Poly(ADP-ribose) polymerase · PVP: Kollidine 17PF-S, [polyvinylpyrrolidone] · STS: Staurosporine · TRD: Taurolidine, [bis-(1,1-dioxoperhydro-1,2,4-thiadiazinyl-4)methane] · VDAC: Voltage-dependent anion channel

Introduction

Taurolidine (TRD) is a synthetic antibiotic and antifungal agent that was first synthesized in the 1970s [6, 7, 21, 29]. In contrast to other compounds, the antibiotic activity of TRD depends upon a chemical reaction secondary to the generation of active TRD catabolites [28, 29] (Fig. 1). Early biochemical and morphological studies revealed that methylol-containing TRD breakdown products directly react with bacterial cell wall components to disrupt their adherence to biological surfaces [18]. This ability of TRD to alter cell surface structure and function is not specific to bacterial cells, and TRD also has been shown to reduce the extent and severity of postoperative peritoneal adhesions. Reflecting these multiple activities, TRD has been administered by lavage after abdominal surgery to reduce postoperative infections and adhesions [4, 6, 7, 34, 35].

We hypothesized that TRD also possesses antineoplastic activity and have reported that this agent inhibits the growth of a variety of human tumor cell lines in vitro [11]. Mechanistic studies, employing PA-1 and SKOV-3 human ovarian tumor cell lines and NIH-3T3 murine fibroblasts, have also revealed that this effect is associated with the induction of apoptosis specifically in tumor cells [11, 23]. We also have evaluated the antineoplastic activity of TRD administered

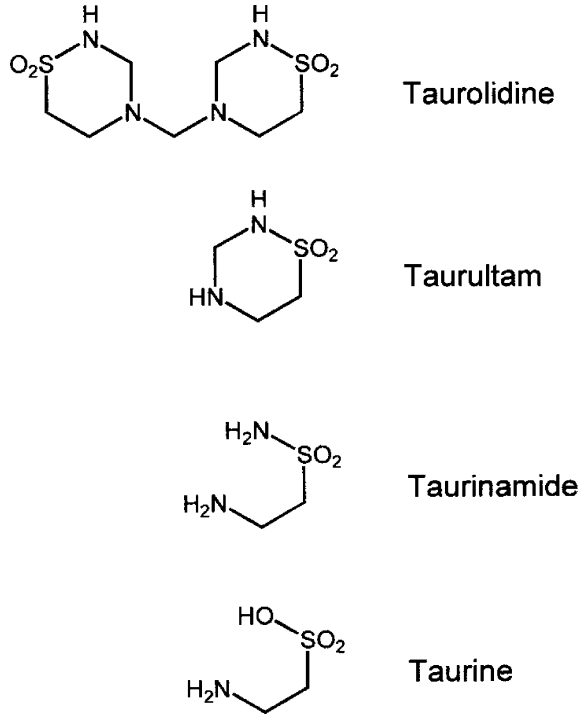

Fig. 1 Structure of TRD and its major breakdown products taurultam, taurinamide and taurine

intraperitoneally (i.p.) in nude female mice bearing i.p. xenografts of human ovarian tumors. Those studies revealed that TRD alone significantly inhibits ovarian tumor formation and growth without the inducing significant toxic effects [11]. This potential antineoplastic activity of TRD also was observed by Jacobi et al., who reported that the i.p. administration of TRD, combined with CO_2 and heparin, can inhibit the formation of peritoneal colon adenocarcinomas in rats following the i.p. administration of DHD/K12 colon adenocarcinoma cells [25, 26]. Similarly, DaCosta et al. and Shrayer et al. have reported that TRD inhibits melanoma cell growth in vitro as well as the development and growth of transplanted melanomas in mice [12, 43].

Our present study was undertaken to further elucidate the mechanism by which TRD induces apoptosis in adherent human prostate tumor cells. We now report that exposing DU145 human prostate tumor cells to TRD induced apoptosis that was associated with the rapid release of cytochrome *c* into the cytoplasm. The release of cytochrome *c* preceded caspase activation and was not blocked by coexposure to the pan-caspase inhibitor zVAD-FMK. Finally, in male nude mice bearing advanced subcutaneous DU145 xenografts, an i.p. (systemic) TRD injection regimen significantly inhibited subcutaneous tumor growth. These results are discussed in light of their biological and therapeutic implications. Preliminary reports of these findings have already been published [10, 15].

Materials and methods

Reagents

TRD was generously provided by Carter Wallace as a 2% solution in 5% PVP (in water). RPMI 1640 cell culture growth medium, trypsin, and fetal bovine serum (FBS) were purchased from GIBCO/Life Technologies. Disposable cell culture flasks and pipettes were obtained from Fisher Scientific. An ApoAlert annexin-V/FITC assay kit was purchased from Clontech. Reagents for SDS-PAGE were from BioRad Laboratories. A murine monoclonal antibody to human PARP was purchased from Zymed Laboratories. A murine monoclonal antibody to cytochrome *c* and a rabbit polyclonal antibody to caspase 8 were from Pharmingen. A rabbit polyclonal antibody to caspase 9 was from Biomol. zVAD-FMK was obtained from Promega Corporation. A murine monoclonal antibody to β-actin as well as all other chemicals were purchased from Sigma.

Cell lines

Mechanistic evaluation of the cytotoxic activity of TRD was carried out in DU-145 human prostate tumor cells. This cell line was obtained from the American Type Culture Collection (ATCC). Cells were cultured in RPMI 1640 medium containing 10% FBS at 37°C in a humidified incubator in an atmosphere containing 5% CO_2. Under these growth conditions, the doubling time of this cell line was about 24 h.

Animals

All studies to assess in vivo toxicity and therapeutic effectiveness were carried out in male homozygous athymic (Hsd/athymic nude nu/nu) mice aged 6–12 weeks obtained from Harlan.

Cell growth inhibition and cytotoxicity assays

Cell growth inhibition. Subconfluent cultures of DU145 cells were harvested by trypsinization and resuspended in medium at a density of $1–5\times10^4$ cells/ml. A 1-ml aliquot of this cell suspension was added to each well of a 12-well cell culture plate that contained 3 ml medium plus serum. TRD was added 24 h later to each well, in a volume of 40 µl to achieve a final concentration of 0–200 μM. Control wells received 40 µl of 5% PVP alone. After a further 72 h, cells were harvested by trypsinization and the cell numbers determined electronically using a Coulter Model Z1 particle counter (Coulter Corporation) to assess cell growth inhibition exactly as previously described [39]. Each experiment was performed in duplicate and repeated a minimum of three times.

Cytotoxicity. DU145 cells (1×10^4) were plated into each well of a 96-well flat-bottom plate (Costar, Corning) in 100 µl RPMI 1640 medium plus 10% FBS. After 24 h, TRD (0–200 µ*M*) was added to each well. After an additional 72 h, 100 µl of a 5 mg/ml MTT solution [3-(4,5-dimethylthiazol-2-yl)-2,5-diphenyltetrazolium bromide] in phosphate-buffered saline (PBS) was added to each well and the plate incubated for 3 h at 37°C. Plates were then centrifuged at 200 *g* for 10 min and the resulting supernatant replaced with 100 µl DMSO. After gently shaking, the absorbance of each well at 550 nm was determined using a Bio-Tek Instruments EL800 plate reader. Cells not exposed to TRD, and medium containing no cells, were used as positive and negative controls, respectively. An absorbance two times that of the negative control was considered positive for the presence of viable cells [41].

Flow cytometry

Cells (2×10^6) were incubated for 24 h in medium containing serum. After 24 h, TRD was added in a volume of 40 µl to achieve a final concentration of 50 or 100 µ*M* (previously determined to be the approximate IC_{50} concentrations after a 24–48 h exposure). Control cultures were incubated in medium containing 40 µl 5% PVP alone. After a further 48 h, all cells were harvested by trypsinization and resuspended in ice-cold PBS at a final cell density of 2×10^6cells/ml. The cells then were stained for 30 min at room temperature in the dark with a solution of 0.05 mg/ml propidium iodide, 0.6% Igepal, and 0.1% sodium citrate. Flow cytometry was performed by FACScan (Becton Dickinson, Plymouth, UK) using the ModFit LT program (Becton Dickinson). Statistical analysis was performed with the Kruskal Wallis non-parametric ANOVA test followed by Dunn's multiple comparisons test using Instat [11].

Cell membrane phosphatidylserine externalization

Cell membrane phosphatidylserine externalization, as a reflection of apoptosis, was assessed by flow cytometry using an ApoAlert annexin-V/FITC assay kit exactly as described by the manufacturer [11, 39]. Briefly, 3×10^5cells were incubated for 24 h in medium containing serum. Thereafter, TRD was added to achieve a final concentration of 50 or 100 µ*M*. Control cultures received 5% PVP alone. Cells were harvested 24 h later by trypsinization, resuspended in 200 µl binding buffer, and incubated for 5–15 min in a solution containing 1 µg/ml annexin-V FITC and 0.0025 mg/ml propidium iodide at room temperature in the dark. The cells were then analyzed to quantitate both annexin-V binding and propidium iodide nuclear staining by cytofluorometric techniques that utilized FACScan using the ModFit LT program with statistical analysis as described above.

Western blot analysis

Cells (2×10^6) were seeded into 75-cm^2 tissue culture flasks containing 20 ml medium plus serum. After 24 h, 100 µ*M* TRD was added. At various times after the addition of TRD, cells were harvested, cell numbers determined, and aliquots containing equal cell numbers generated from each exposure condition. Total proteins from these aliquots were separated by SDS-PAGE and transferred to nitrocellulose filters. Filters were processed and probed with appropriate antibodies to detect procaspases 8 or 9 or PARP. The resulting protein–antibody complexes were visualized by chemiluminescence techniques [14, 16]. Parallel studies were conducted in which cells were simultaneously exposed to 100 µ*M* TRD plus 20 µ*M* of the pan-caspase inhibitor zVAD-FMK [2, 5, 24] and then processed for Western blot analysis as described above.

Cytochrome *c* in the mitochondrion-free cytoplasmic fraction of cells treated as described above also was assessed by Western blotting. Specifically, DU145 cells were incubated in medium containing 100 µ*M* TRD. At selected times thereafter, $1.5–2.0\times10^7$ cells were harvested by trypsinization and resuspended in ice-cold isolation buffer (250 m *M* sucrose, 20 m *M*Hepes, 10 m *M* KCl, 1.5 m *M* $MgCl_2$, 1 m *M* EDTA, 1 m *M* EGTA, pH 7.4) for 15 min. Thereafter, cells were gently disrupted using a Dounce homogenizer and unlysed cells, intact nuclei and mitochondria were removed by centrifugation at 10,000 *g* for 25 min. The resulting supernatant, representing the mitochondrion-free cytoplasmic fraction, was then processed for Western blot analysis, exactly as described above.

In vivo evaluation of toxicity and therapeutic effectiveness

To evaluate potential TRD-induced toxicity, mice were divided into groups of five to eight animals, weighed and three weekly cycles of TRD therapy initiated. Each cycle consisted of three single i.p. bolus injections, administered as one injection per day on three alternate days per week (i.e., Monday, Wednesday, Friday). TRD doses ranged from 500 to 700 mg/kg per day. Control animals received i.p. injections of 5% PVP alone on three alternate days per week. Animals were examined daily and body weight recorded twice weekly. A reduction in body weight of greater than 10% was considered significant. The MTD regimen was identified as that producing about 10% mortality 1 week after the completion of treatment [8, 11, 13].

To evaluate therapeutic effectiveness, mice received a single subcutaneous injection into the left axillary region of 5×10^6 DU145 cells in a volume of 0.5 ml. Mice then were examined daily. When the resulting tumors were palpable, the tumor size in each mouse was determined by external caliper measurement and tumor weight estimated using the formula: weight (mg) = [width

$(mm)]^2 \times$ length (mm)/2 [8, 13]. Mice then were distributed into treatment groups of seven to ten animals so that each group had approximately the same mean tumor weight. Immediately thereafter mice were weighed and the first cycle of TRD therapy initiated employing the MTD regimen identified above (so as to allow comparisons of antineoplastic activity with other agents/regimens under equitoxic conditions). Animals were examined daily and body weight and tumor size recorded twice weekly. Two weeks following the last TRD injection mice in all groups were killed by CO_2 asphyxiation. Differences in the mean tumor weight between treatment groups at each measurement point were evaluated statistically using Student's *t*-test with *P*values of ≤ 0.05 considered significant [8, 11].

Results

The antiproliferative activity of TRD in DU145 cells following a 3-day exposure was assessed and the IC_{50} was about 10 μM. To determine if this growth-inhibitory effect was a reflection of cytotoxicity, in parallel studies the IC_{50} following a 3-day exposure was determined using 3-(4,5-dimethylthiazol-2-yl)-2,5-diphenyltetrazolium bromide as a marker of mitochondrial function. The results of this study supported those obtained from the antiproliferation studies, and revealed that this 3-day exposure to TRD was cytotoxic with an IC_{50} of about 16.8 μM.

We have reported that, in alternate tumor cell models [11, 23], TRD exposure results in cellular changes that appear to reflect TRD-induced apoptosis. Therefore, the effects of a 48-h TRD exposure on the appearance of DNA debris in the sub-G_0/G_1 region of the cell cycle were next assessed. This study revealed that drug exposure induced a significant increase in DNA debris in the sub-G_0/G_1 region (Fig. 2). Parallel studies to assess the effect of TRD on membrane phosphatidylserine externalization indicated that a 24-h drug exposure also induced a significant increase in annexin-V binding without a concomitant increase in propidium iodide staining (Fig. 2). The ability of TRD to induce both DNA fragmentation and phosphatidylserine externalization suggests that these human prostate tumor cells also undergo apoptosis as a consequence of drug exposure. This possibility was confirmed by assessing the effect of TRD on PARP cleavage [11, 31, 44]. Western blot analysis, carried out on whole cell extracts of DU145 cells following a 12-h exposure to 100 μM TRD, revealed cleavage of this nuclear protein under these conditions (Fig. 3). Concomitant studies in cells exposed to both TRD and the pan-caspase inhibitor zVAD-FMK [2, 5, 24] demonstrated that, under these conditions, PARP cleavage was prevented (Fig. 3). These findings confirmed that, as observed in HL60 leukemic cells, TRD-induced apoptosis was caspase mediated in this solid tumor model [23].

The two predominant apoptotic processes in tumor cells are defined as either receptor-mediated (extrinsic pathway) or mitochondrial-mediated (intrinsic pathway) [19, 27, 38]. In the receptor-mediated process, cell death is initiated by ligand binding to specific membrane receptors, such as CD95, that lead to the formation of death-inducing signaling complex (DISC) and the activation of the apical procaspases 8 and/or 10 [3, 9, 19, 20, 36, 46]. In mitochondrial-mediated apoptosis the initiating event is variable but leads to mitochondrial

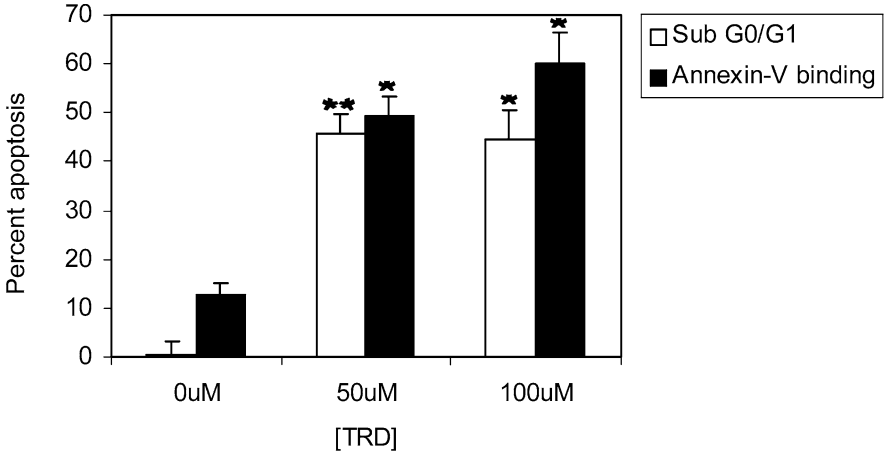

Fig. 2 TRD triggers apoptosis in DU145 cells. *Open bars* The effect of a 48-h exposure to TRD on the appearance of DNA debris in the sub-G_0/G_1 region of the cell cycle in DU145 cells. DU145 cells were incubated in medium containing TRD at a final concentration of 50 or 100 μM. Control cultures were incubated in medium containing 40 µl 5% PVP alone. After 48 h, cells were harvested by trypsinization and processed. Flow cytometry was performed by FACScan and data analyzed using the ModFit LT program [13]. Data from individual treatment groups were pooled for statistical analysis. *Solid bars* The effect of a 24-h exposure to TRD on membrane phosphatidylserine externalization in DU145 cells. Cells were incubated for 24 h in medium containing TRD at a final concentration of 50 or 100 μM. Control cultures were incubated in medium containing 40 µl 5% PVP alone. Cells were then harvested and phosphatidylserine externalization determined by assessing annexin-V FITC binding and concomitant propidium iodide staining using cytofluorometric techniques. Data from individual treatment groups were pooled for statistical analysis. Each bar represents the mean ± SE of four to six determinations. $*P \leq 0.01$, $**P \leq 0.001$ (vs nontreated control)

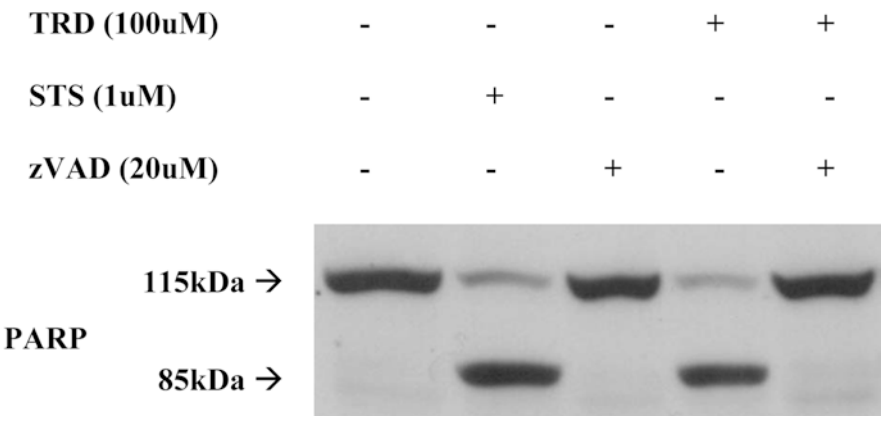

Fig. 3 TRD-induced PARP cleavage is caspase dependent. Typical results from Western blot analysis of the effect of a 12-h exposure to 100 μ*M* TRD, 1 μ*M* STS, or 20 μ*M*zVAD-FMK on PARP expression and the appearance of a major PARP cleavage product in DU145 human prostate tumor cells. Cells (2×10^6) were seeded in 75-cm^2 tissue culture flasks, and 24 h later TRD, STS, or zVAD-FMK were added at the noted concentrations. After an additional 12 h, cells were harvested and aliquots containing equal amounts of protein generated from each exposure condition. Total proteins from these lysates were separated by SDS-PAGE and transferred to nitrocellulose filters. Filters were then immunoblotted to detect intact PARP protein and cleavage fragments. The resulting protein–antibody complexes were visualized by chemiluminescence techniques [14, 16]

membrane permeabilization, the release of cytochrome *c*, activation of Apaf-1, and subsequent activation of procaspase 9, the apical caspase in this apoptotic pathway [1, 9, 22, 30, 32, 45, 47]. Both intrinsic and extrinsic apoptosis results in the activation of executioner caspases, such as caspase 3, and eventual cleavage of target proteins such as PARP [9]. We have observed that in a non-adherent human promyelocytic leukemia cell line TRD-induced apoptosis is associated with procaspase 9 activation and cytochrome *c*efflux from mitochondria [23, 40], thus supporting the contention that, in these cells, TRD exposure activates the intrinsic apoptotic pathway.

Parallel experiments in the present study were designed to identify the apical caspases activated following TRD exposure. Cells were incubated in medium containing 100 μ*M* TRD. At 1-h intervals cells were harvested, mitochondria removed, and the resulting mitochondrion-free cytosol fraction prepared for Western blot analysis to assess the temporal progression of procaspase 8 and caspase 9 activation as well as cytochrome *c* release from mitochondria. The results of this analysis are presented in Fig. 4. Procaspase 9 activation, as defined by the appearance of the p35 and p37 fragments, appeared to occur within 2 h of TRD exposure. Following TRD exposure procaspase 8 also was activated, leading to the appearance of the p41 and p43 fragments. However, Western blot analysis showed that the activation of this caspase appeared to occur 3–4 h after TRD exposure and subsequent to the activation of procaspase 9. Assessment of the temporal relationship between TRD exposure and the appearance of cytochrome *c* in the cytoplasm revealed that within 1 h following drug exposure extra-mitochondrial cytochrome *c* could be detected.

To confirm the apical position of cytochrome *c* efflux in this TRD-induced sequence of events, complementary experiments to those described above were carried out in the presence of TRD and zVAD-FMK. As expected, in the presence of this pan-caspase inhibitor activation of both procaspase 8 and procaspase 9 was inhibited (Fig. 5). Nevertheless, in the presence of zVAD, exposure to TRD resulted in the appearance of cytochrome *c* in the mitochondrion-free cytosolic fraction (Fig. 5). These results suggest that TRD exposure resulted in rapid mitochondrial membrane permeabilization and release of cytochrome *c* that was followed by the initiation of a caspase 9-mediated apoptotic cascade (intrinsic apoptotic pathway) [22].

The results supported the contention that TRD possessed antineoplastic activity in this model of human prostate cancer. Studies next were conducted in male nude mice bearing xenografts of DU145 human prostate tumor cells to directly test this possibility. Unlike previous studies in which TRD was administered i.p. to animals bearing i.p. tumors, the present study was designed to determine if TRD possessed systemic antineoplastic activity against a distant tumor mass. Initially, the toxicity generated by up to three cycles of TRD, with each cycle comprising one i.p. bolus injection administered to each of three alternate days per week, was assessed. Based on previous findings [11], the doses tested were 500, 600, and 700 mg/kg per injection (corresponding to 1500, 1800, and 2100 mg/kg per week, respectively). All three dosage regimens induced dose-dependent toxicity after the first cycle (Table 1). If this regimen was repeated weekly for a total of three cycles, whole-animal toxicity, as measured both by body weight loss and mortality, continued to increase in a dose-dependent manner (Table 1). Following three cycles of therapy the 500 mg/kg per injection regimen produced a maximal body weight loss of about 14%, and mortality of $<8\%$ and was identified as the MTD regimen. We next assessed the antineoplastic activity of three cycles of the 500 mg/kg per injection regimen. For these studies,

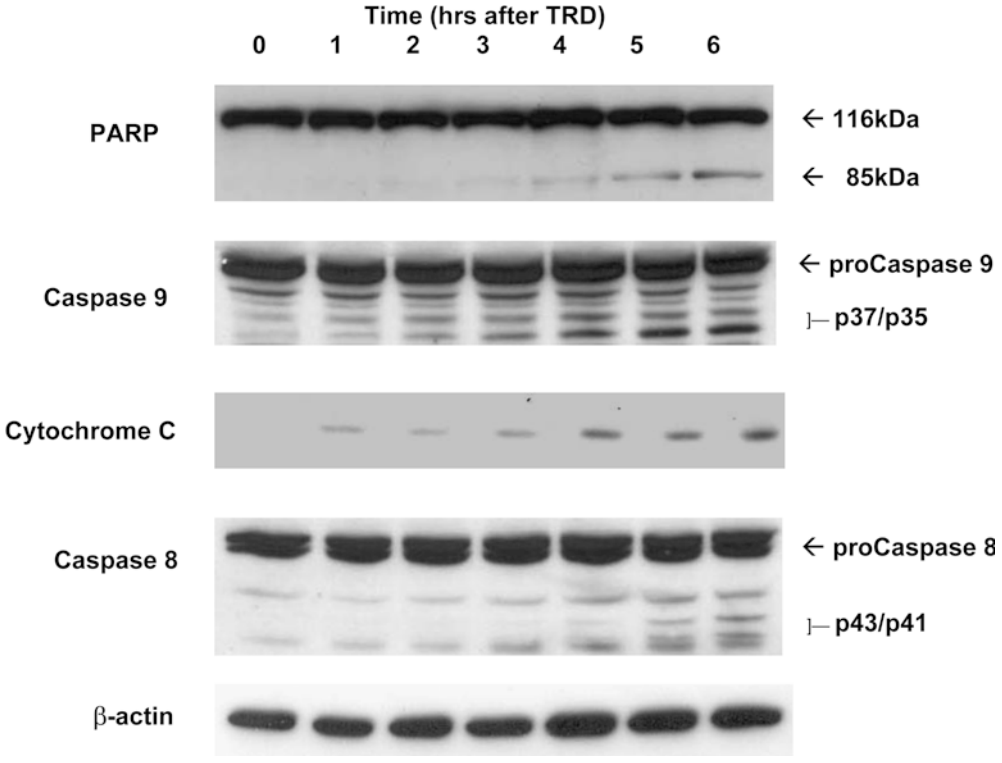

Fig. 4 TRD-induced apoptosis is associated with the activation of procaspase 8, procaspase 9 and the release of cytochrome *c* from mitochondria. Typical results of Western blot analysis of the effects of exposure for 0–6 h to 100 μ*M* TRD on procaspase 8 and procaspase 9 expression and the appearance of cytochrome *c* in the cytoplasm of DU145 human prostate tumor cells are shown. Cells (2×10^6) were seeded in 75-cm^2 tissue culture flasks, and 24 h later were exposed to 100 μ*M* TRD. At hourly intervals thereafter cells were harvested, lysed, large cell debris and mitochondria removed by centrifugation, and cytoplasmic aliquots, containing equal amounts of protein, generated from each time point. Total proteins from these cytosolic fractions were separated by SDS-PAGE and transferred to nitrocellulose filters. Filters were then immunoblotted to detect procaspase 9, procaspase 8, and cytochrome *c*. The resulting protein–antibody complexes were visualized as described in Fig. 3

mice were injected subcutaneously into the left axillary region with DU145 cells and TRD therapy was initiated when the resulting xenografts were palpable. The ability of this TRD regimen to inhibit xenograft growth is summarized in Fig. 6 that compares tumor growth as a function of time in both treated and control mice. During the course of treatment, this TRD regimen significantly inhibited tumor growth compared to that in PVP-treated control animals.

Discussion

We have reported that TRD exposure results in apoptosis in human ovarian tumor cells and in human promyelocytic leukemia cells and that this effect can be exploited for therapeutic advantage [11, 23]. To expand upon those findings, the present study was carried out to assess the cytotoxic and antineoplastic activity of TRD in the DU145 human prostate tumor model. We now report that, in this model also, TRD exposure resulted in tumor cell death that reflected the induction of apoptosis. Furthermore, our present results revealed that exposure to TRD induced intrinsic, mitochondrial-mediated, apoptosis in these androgen-insensitive human prostate tumor cells. This effect was associated with mitochondrial membrane permeabilization reflected by cytochrome *c* efflux into the cytoplasm, an event preceding caspase activation.

The mechanistic basis of this ability of TRD to induce cellular effects leading to mitochondrial depolarization, release of cytochrome *c* and activation of procaspase 9 is yet to be identified. In the present study, coexposing DU145 cells to both TRD and zVAD-FMK did not block cytochrome *c*efflux, indicating that this mitochondrial effect preceded caspase activation. This could suggest that TRD, or a TRD metabolite, directly affected mitochondrial membrane stability. Specifically, TRD or one of its breakdown products might affect either the voltage-dependent anion channel (VDAC) or the adenine nucleotide transporter (ANT). The VDAC is an abundantly expressed outer mitochondrial membrane protein. Disruption of the VDAC has been reported to be required for the induction of apoptosis [18] and directly leads to cytochrome *c* efflux. Furthermore, this effect can be blocked and the VDAC stabilized by Bcl-2 [45]. Of interest, we have reported that Bcl-2 overexpression inhibits the proapoptotic activity of TRD in HL60 cells [17, 23]. Similarly, the ANT is an abundantly expressed inner mitochondrial membrane protein that can directly interact with the VDAC to influence the movement of proteins across the mitochondrial mem-

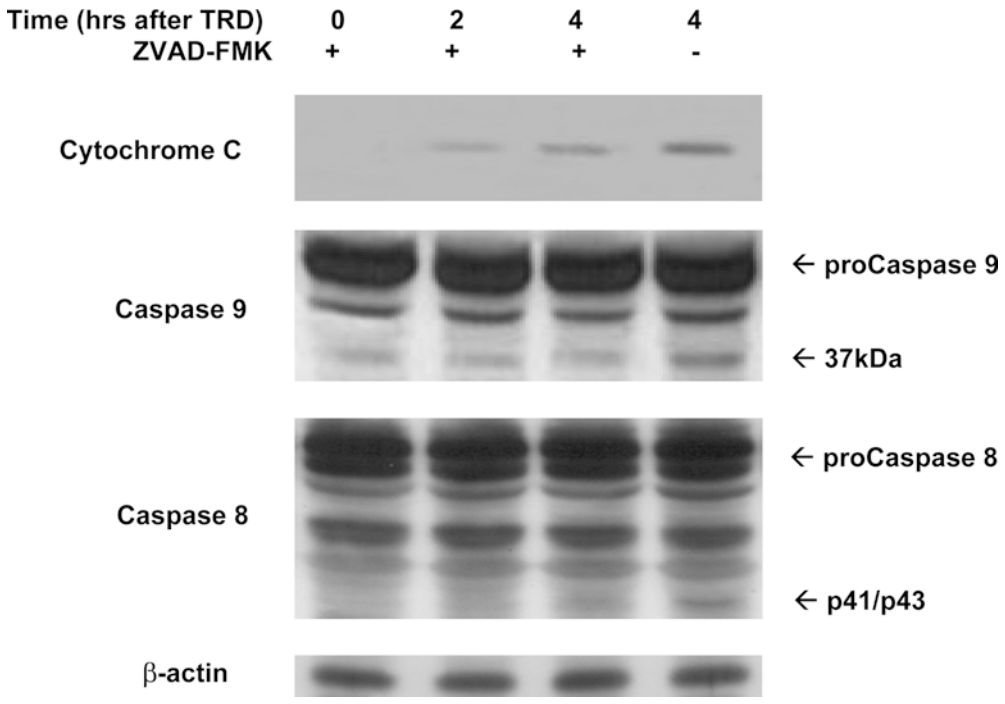

Fig. 5 TRD-induced cytochrome *c* release is independent of caspase activity. Typical results from Western blot analysis of the effects of exposure for 0–4 h to 100 μ*M* TRD plus 20 μ*M*zVAD-FMK on procaspase 8 and procaspase 9 expression and the appearance of cytochrome *c* in the cytoplasm in DU145 human prostate tumor cells are shown. Cells (2×10^6) were seeded in 75-cm^2 tissue culture flasks. The cells were exposed 24 h later to 20 μ*M* zVAD-FMK and 30 min later to 100 μ*M* TRD. At the noted times thereafter, the cells were harvested, lysed, large cell debris and mitochondria removed by centrifugation, and aliquots of the remaining supernatant, containing an equal amount of protein, generated from each harvest time point. Total proteins from these aliquots were separated and analyzed exactly as described in Fig. 4

branes [17, 37]. Normal ANT function is dependent upon Ca^{2+} homeostasis and Ca^{2+} flux can lead to ANT dysfunction and apoptosis [33, 42]. Since it has been reported that changes in the intracellular concentration of the amino acid taurine can disrupt Ca^{2+} homeostasis, it is intriguing to speculate that a TRD breakdown product disrupts Ca^{2+}homeostasis and thus affects mitochondrial membrane permeability. Using a cell-free mitochondrial assay system, studies are underway to determine if TRD, or one of its major metabolites, directly affects mitochondrial membrane permeability.

Alternatively, the effect of TRD on cytochrome *c* efflux may be indirect. In this case, TRD may affect signaling through, for example, the AKT pathway. This could lead to a reduction in Bad phosphorylation, mitochondrial membrane destabilization, and, ultimately, cytochrome *c* efflux. This possibility also is supported by our previous finding that TRD-induced apoptosis is abrogated by overexpression of the apoptosis suppressor Bcl-2 [23]. Preliminary studies are underway to determine if exposure to TRD alters PI3 kinase phosphorylation and/or activity as reflected by the phosphorylation status of AKT.

Table 1 TRD-induced toxicity in athymic (nude) male mice. Groups of five to ten mice were treated with three cycles of TRD therapy, each cycle comprising three i.p. TRD injections, administered as one injection per day on three alternate days per week (i.e., Monday, Wednesday, Friday). Doses ranged from 500 to 700 mg/kg per injection and were delivered in a volume of $\leq$ 1.5 ml. During the injection regimen mice were examined daily and body weight recorded twice weekly. Experiments were repeated a minimum of three times and mortality and weight loss data pooled

Cycle[a]	TRD dose (mg/kg per injection)	*n*[b]	Weight loss (nadir %)	Mortality (%)
1	None (vehicle control)	28	−1.9	0
	500	27	−5.0	0
	600	29	−8.6	3.4
	700	30	−9.3	6.7
2	None (vehicle control)	28	−1.9	0
	500	26	−8.5	3.7
	600	26	−12.6	10.3
	700	23	−15.6	23.3
3	None (vehicle control)	28	−8.7	0
	500	25	−14.4	7.4
	600	18	−16.8	37.9
	700	15	−19.6	50.0

[a]One cycle consisted of three i.p. injections of TRD administered as one injection per day on alternate days per week (i.e., Monday, Wednesday, Friday)
[b]Total number of animals treated in that cycle at that dose

Regardless of the exact mechanism(s) ultimately found to be responsible for TRD-induced death in various tumor cell models, it remains remarkable that exposure conditions resulting in apoptosis in tumor cell lines are not cytotoxic in fibroblasts or normal marrow

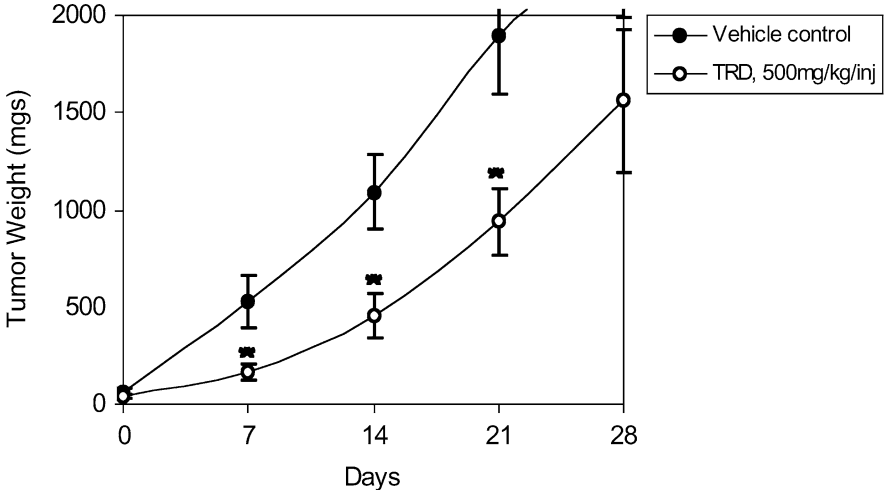

Fig. 6 The effect of three cycles of TRD therapy on the growth of advanced subcutaneous xenografts of DU145 human prostate tumor cells in athymic (nude) male mice. Mice received a single subcutaneous injection into the left axillary region of 5×10^6 DU145 cells in a volume of 0.5 ml. When the resulting tumors were palpable, mice were distributed into treatment groups of seven to ten animals such that each group had approximately the same mean tumor weight. Immediately thereafter mice were weighed and the first of three weekly cycles of TRD therapy started. Animals were examined daily. Body weight and xenograft tumor dimensions were recorded twice weekly. Mice in all groups were killed by CO_2 asphyxiation 14 days following the last TRD injection. Each experiment was repeated three times and the pooled number of animals in each treatment group was 28–30 [8, 13]. The results are presented as the means ± SE. $^*P \leq 0.01$

[11, 41]. Preclinically, in selected rodent models of peritoneal tumor growth, the i.p. administration of TRD has been found to significantly inhibit tumor formation and growth [11, 12, 23, 25, 26]. In the present study, the i.p. administration of TRD was found to inhibit the growth of distant subcutaneous solid tumor xenografts. This supports the findings of DaCosta et al. that i.p. TRD inhibited the growth of subcutaneous B16 melanoma in mice [12]. These authors speculated that, in this model, TRD did not directly affect B16 tumor cells but rather exerted an immunostimulatory effect that affected LAK cell and NK cell activity. While this reported effect of TRD on immune function may be relevant, in the present study, antineoplastic activity was observed in immunosuppressed athymic nude mice, suggesting a more direct effect of TRD on tumor cells. The possibility of a direct interaction between TRD (or one of its metabolites) and tumor cells is supported further by our finding that TRD selectively kills tumor cells in vitro [11, 41]. In vivo studies also are underway to correlate the tumor cell killing activity of TRD with exposure to either the parent molecule or its major metabolites. It is anticipated that the results of these studies will help further refine TRD dosage regimens as well as facilitate studies to identify the mechanism(s) by which exposure to this agent induce tumor cell death in vivo.

In total, the results of these related studies support our position that TRD, or one of its metabolites, exerts a direct cytotoxic effect on tumor cells and thus possesses exploitable clinical utility in the treatment of human cancer. To test this possibility we have initiated a series of phase I and II clinical trials in patients with advanced ovarian cancer and recurrent glioblastoma multiforme. Preliminary results from these trials reveal that both i.p. and intravenous administration of TRD at 20 g/day is well tolerated. Reflecting its low clinical toxicity and highly tumor cell-specific effects, further laboratory and clinical evaluation of this novel antineoplastic agent is warranted.

Acknowledgments Supported by Carter-Wallace, Inc., The T. J. Martell Foundation, and Rhode Island Hospital.

References

1. Adams JM, Huang DC, Puthalakath H, Bouillet P, Vairo G, Moriishi K, Hausmann G, O'Reilly L, Newton K, Ogilvy S, Bath ML, Print CG, Harris AW, Strasser A, Cory S (1999) Control of apoptosis in hematopoietic cells by the cl-2 family of proteins. Cold Spring Harb Symp Quant Biol 64:351–358
2. Atkinson EA, Barry M, Darmon AJ, Shostak I, Turner PC, Moyer RW, Bleackley RC (1998) Cytotoxic T lymphocyte-assisted suicide. Caspase 3 activation is primarily the result of a direct action of granzyme B. J Biol Chem 273:21261–21266
3. Bantel H, Engels IH, Voelter W, Schulze-Osthoff K, Wesselborg S (1999) Mistletoe lectin activates caspase-8/FLICE independently of death receptor signaling and enhances anticancer drug-induced apoptosis. Cancer Res 59:2083–2090
4. Blenkharn JI (1987) The antibacterial and antiendotoxin activity of taurolidine in combination with antibiotics. Surg Res Commun 2:149–155
5. Bossey-Wetzel E, Newmeyer DD, Green DR (1998) Mitochondrial cytochrome c release in apoptosis occurs upstream of DEVD-specific caspase activation and independently of mitochondrial transmembrane depolarization. EMBO J 17:37–49
6. Browne MK, Leslie GB, Pfirrmann RW, Brodhuge H (1977) The in vitro and in vivo activity of taurolin against anaerobic pathogenic organisms. Surg Gynecol Obstet 145:842–846
7. Browne MK, Mackenzie M, Doyle PJ (1978) A controlled trial of taurolin in established bacterial peritonitis. Surg Gynecol Obstet 146:721–724

8. Brunetti I, Falcone A, Calabresi P, Goulette FA, Darnowski JW (1990) 5-Fluorouracil enhances azidothymidine cytotoxicity: in vitro, in vivo, and biochemical studies. Cancer Res 50:4026–4031
9. Budijardjo I, Oliver H, Lutter M, Luo X, Wang X (1999) Biochemical pathways of caspase activation during apoptosis. Annu Rev Cell Dev Biol 15:269–290
10. Calabresi P, Goulette FA, Darnowski JW (2000) Antineoplastic effects of taurolidine in human tumor cell lines. Proc Am Assoc Cancer Res 41:771
11. Calabresi P, Goulette FA, Darnowski JW (2001) Taurolidine: cytotoxic and mechanistic evaluation of a novel antineoplastic agent. Cancer Res 61:6816–6821
12. DaCosta ML, Redmond HP, Bouchier-Hayes DJ (2001) Taurolidine improves survival by abrogating the accelerated development and proliferation of solid tumors and development of organ metastases from circulating tumor cells released following surgery. J Surg Res 101:111–119
13. Darnowski JW, Handschumacher RE (1985) Tissue-specific enhancement of uridine utilization and 5-fluorouracil therapy in mice by benzylacyclouridine. Cancer Res 45:5364–5368
14. Darnowski JW, Davol PA, Goulette FA (1997) Human recombinant interferon alpha-2a plus 3′-azido-3′-deoxythymidine. Synergistic growth inhibition with evidence of impaired DNA repair in human colon adenocarcinoma cells. Biochem Pharmacol 53:571–580
15. Darnowski JW, Goulette FA, Wagner EF, Simms E, Calabresi P (2001) Taurolidine: a novel, nontoxic, antineoplastic agent that induces apoptosis in androgen-independent DU145 human prostate tumor cells. Proc Am Assoc Cancer Res 42:212
16. Davol PA, Goulette FA, Frackelton AR Jr, Darnowski JW (1996) Modulation of p53 expression by human recombinant interferon-a2a correlates with abrogation of cisplatin resistance in a human melanoma cell line. Cancer Res 56:2522–2526
17. Debatin KM, Poncet D, Kroemer G (2002) Chemotherapy: targeting the mitochondrial cell death pathway. Oncogene 21:8786–8803
18. Erb F, Imbenotte M, Huveene J (1983) Structural investigation of a new organic antimicrobial: taurolidine. Analytical study and application to identification and quantification in biological fluids. Eur J Drug Metabol Pharmacokinet 8:163–173
19. Fulda S, Sievens H, Frieson C, Herr I, Debatin KM (1997) The CD95 (APO-1/Fas) system mediates drug-induced apoptosis in neuroblastoma cells. Cancer Res 57:3823–3829
20. Fulda S, Frriesen C, Los M, Scaffidi C, Mier W, Benedict M, Nunez G, Krammer PH, Peter ME, Debatin KM (1997) Botulinic acid triggers CD95 (APO-1/Fas)- and p53-independent apoptosis via activation of caspases in neuroectodermal tumors. Cancer Res 57:4956–4965
21. Gorman SP, McCafferty DF, Woolfson AD, Junes DS (1987) Reduced adherence of microorganisms to human mucosal epithelial cells following treatment with taurolin, a novel antimicrobial agent. J Appl Bacteriol 62:315–320
22. Green DR, Kroemer G (1998) The central executioners of apoptosis: caspases or mitochondria? Trends Cell Biol 8:267–271
23. Han Z, Ribizzi I, Pantazis P, Wyche JH, Darnowski J, Calabresi P (2002) The antibacterial drug taurolidine induces apoptosis by a mitochondrial cytochrome c-dependent mechanism. Anticancer Res 22:1959–1964
24. Hartfield PJ, Bilney AJ, Murray AW (1998) Neurotrophic factors prevent ceramide-induced apoptosis downstream of c-Jun N-terminal kinase activation in PC12 cells. J Neurochem 71:161–169
25. Jacobi CA, Ordemann J, Bohm B, Zieren HU, Sabat R, Muller JM (1997) Inhibition of peritoneal tumor cell growth and implantation in laparoscopic surgery in a rat model. Am J Surg 174:359–363
26. Jacobi CA, Wildbrett P, Volk T, Muller JM (1999) Influence of different gases and intraperitoneal instillation of antiadherent or cytotoxic agents on peritoneal tumor cell growth and implantation with laparoscopic surgery in a rat model. Surg Endosc 13:1021–1025
27. Kasibhatla S, Brunner T, Genestier L, Echeverri F, Mahboubi A, Green DR (1998) DNA damaging agents induce expression of Fas ligand and subsequent apoptosis in T lymphocytes via activation of NF-KB and AP-1. Mol Cell 1:543–551
28. Knight BI, Skellern GG, Browne MK, Pfirrmann RW (1981) The characterization and quantitation by HPLC (high performance liquid chromatography) of the metabolites of taurolin. Br J Clin Pharmacol 12:439–440
29. Knight BI, Skellern GG, Smail GA, Browne MK, Pfirrmann RW (1983) NMR studies and GC analysis of the antibacterial agent, taurolidine. J Pharm Sci 72:705–707
30. Kuida K (2000) Caspase-9. Int J Biochem Cell Biol 32:121–124
31. Lazebnik YA, Kaufmann SH, Desnoyers S, Poirier GG, Earnshaw WC (1994) Cleavage of poly (ADP-ribose) polymerase by a proteinase with properties like ICE. Nature 371:346–347
32. Li P, Nijhawan D, Budihardjo I, Srinivasula SM, Ahmed M, Alnemri ES, Wang X (1997) Cytochrome c and dATP-dependent formation of Apaf-1/caspase-9 complex initiates an apoptotic protease cascade. Cell 91:479–489
33. Magalhaes PJ, Rizzuto R (2001) Mitochondria and calcium homeostasis: a tale of three luminescent proteins. Luminescence 16:67–71
34. McCartney AC, Browne MK (1988) Clinical studies on administration of taurolin in severe sepsis: a preliminary study. Prog Clin Biol Res 272:361–371
35. Moser G, Martin MD (1978) Forty cases of peritonitis treated without antibiotics: the intraperitoneal and intravenous use of taurolin. PRAXIS 67:425–428
36. Muller M, Strand S, Hug H, Heinemann EM, Walczak H, Hoffman WJ, Stremmel W, Krammer PH, Galle PR (1997) Drug-induced apoptosis in hepatoma cells is mediated by CD95 (APO-1/Fas) receptor/ligand system and involves activation of wild-type p53. J Clin Invest 99:403–413
37. Newmeyer DD, Ferguson-Miller S (2002) Mitochondria: releasing power for life and unleashing the machineries of death. Cell 112:481–490
38. Petak I, Tillman DM, Harwood FG, Mihalik R, Houghton JA (2000) Fas-dependent and -independent mechanisms of cell death following DNA damage in human colon carcinoma cells. Cancer Res 60:2643–2650
39. Ribizzi I, Darnowski JW, Goulette FA, Sertoli MR, Calabresi P (2000) Amifostine cytotoxicity and induction of apoptosis in a human myelodysplastic cell line. Leuk Res 24:519–525
40. Ribizzi I, Han Z, Darnowski JW, Goulette F, Wagner EF, Calabresi P (2001) Taurolidine: mechanism of action of a novel and safe cytotoxic agent for cancer therapy. Proc Am Assoc Cancer Res 42:212
41. Ribizzi I, Darnowski JW, Goulette FA, Akhtar MS, Chatterjee D, Calabresi P (2002) Taurolidine: preclinical evaluation of a novel, highly selective, agent for bone marrow purging. Bone Marrow Transplant 29:313–319
42. Rizzuto R, Bernardi P, Pozzan T (2000) Mitochondria as all-around players of the calcium game. J Physiol 529:37–47
43. Shrayer DP, Lukoff H, King T, Calabresi P (2003) The effect of taurolidine on adherent and floating subpopulations of melanoma cells. Anticancer Drugs 14:295–303
44. Smulson ME, Pang D, Jung M, Dimtchev A, Chasovskikh S, Spoonde A, Simbulan-Rosenthal C, Rosenthal D, Yakovlev A, Dritschilo A (1998) Irreversible binding of poly (ADP-ribose) polymerase cleavage product to DNA ends revealed by atomic force microscopy: possible role in apoptosis. Cancer Res 58:3496–3498

45. Wei MC, Zong WX, Cheng EH, Linsten T, Panoutsakopoulou V, Ross AJ, Roth KA, MacGregor GR, Thompson CB, Korsmeyer SJ (2001) Proapoptotic BAX and BAK: a requisite gateway to mitochondrial dysfunction and death. Science 292:727–730
46. Wesselborg S, Engels IH, Rossman E, Los M, Schulze-Osthoff K (1999) Anticancer drugs induce caspase-8/FLICE activation and apoptosis in the absence of CD95 receptor/ligand interaction. Blood 93:3053–3063
47. Zou H, Li X, Wang X (1999) An APAF-1 cytochrome c multimeric complex is a functional apoptosome that activates procaspase-9. J Biol Chem 274:11549–11556